Synthesis of hierarchically porous inorganic–metal site-isolated nanocomposites†

Haifei Zhang,*[a] Irshad Hussain,[ab] Mathias Brust[a] and Andrew I. Cooper[a]

Received (in Cambridge, UK) 27th March 2006, Accepted 21st April 2006
First published as an Advance Article on the web 9th May 2006
DOI: 10.1039/b604392e

Hierarchically porous inorganic nanocomposites have been synthesized combining interconnected macropores and mesopores with a high loading of site-isolated gold nanoparticles.

The investigation of nanoparticles for heterogeneous catalysis is an area of continued interest. Nanoparticles are very often supported within mesoporous metal oxides such as silica, alumina, or titania. There are a number of methods to prepare nanoparticle-functionalized porous materials. For example, metal organic clusters can be impregnated into a porous substrate and followed by the *in situ* formation of metal nanoparticles by thermal decomposition.[1,2] A deposition–precipitation (DP) method was used to prepare nanoparticles supported on porous metal oxides by the deposition of precursors followed by calcination.[3] Gold nanoparticles are relatively easy to prepare and have significant stability in air, even in the nanodispersed state.[4,5] As such, an alternative preparative route for gold nanocomposites is to first prepare the nanoparticles and then to incorporate these particles into a porous substrate by some means.[6]

Exclusively microporous or mesoporous supports exhibit high surface areas but may suffer from diffusion limitations in applications such as liquid phase catalysis. The introduction of interconnected macropores in the support may enhance mass transport, particularly for viscous systems or for large molecules (*e.g.* biomacromolecules). For example, colloidal assemblies have been used as templates to prepare materials in which metal nanoparticles are doped into macroporous carbon[7] and ordered macroporous solids.[6] However, the loading of preformed nanoparticles into porous materials in a stable, non-aggregated state remains a significant challenge.[8]

A versatile route for the preparation of macroporous materials is emulsion templating, where the internal droplet phase acts as a template for the macropores.[9,10] In this communication, we have used macroporous emulsion-templated polyacrylamide (PAM) beads as templates to prepare hierarchically-porous inorganic beads with a high loading of discrete gold nanoparticles. Gold nanoparticles (GNPs) were used as a model because of their high stability to oxidation and potential use as a catalyst for the oxidation of alkenes.[11,12] The materials that we have produced combine emulsion-templated macropores (>5 μm) interconnected with mesopores (2–10 nm) that are generated by the sol–gel process. Hierarchical porosity of this type is an important goal for support materials in certain catalytic processes.[13]

The process for preparing these hierarchically porous GNP–silica composites is summarized in Fig. 1.

First, highly macroporous PAM beads were prepared by "oil-in-water-in-oil" (O/W/O) sedimentation polymerization.[10] (It should be noted that other morphologies of PAM could also be used in the following process).[9b] An aqueous sodium acrylate-stabilized gold nanodispersion was prepared as described previously.[5] It was found that sodium acrylate-stabilized gold nanoparticles could be adsorbed irreversibly onto the porous PAM beads, as in the preparation of macroporous metallic gold structures.[14] As a result, the red GNP aqueous dispersion was decolourised and the white PAM beads became red in colour. The adsorption process took about seven days to achieve a high loading of GNPs on the polymer structure, even though a concentrated nanodispersion was used in order to maximise the loading speed. It was then possible to produce emulsion-templated metallic gold beads by removal of the PAM phase by calcination.[14] Under such conditions, the GNPs fuse together indistinguishably to produce macroporous bulk metallic gold with a relatively low surface area.[14] In this new study, the PAM beads were soaked in a GNP solution at a concentration of 1.5 g L^{-1}. Using this procedure, the PAM beads were loaded with approximately 15 wt% gold. The red GNP–PAM composite beads were then soaked in a silica sol and kept in a freezer at −20 °C overnight. After incubating the material at

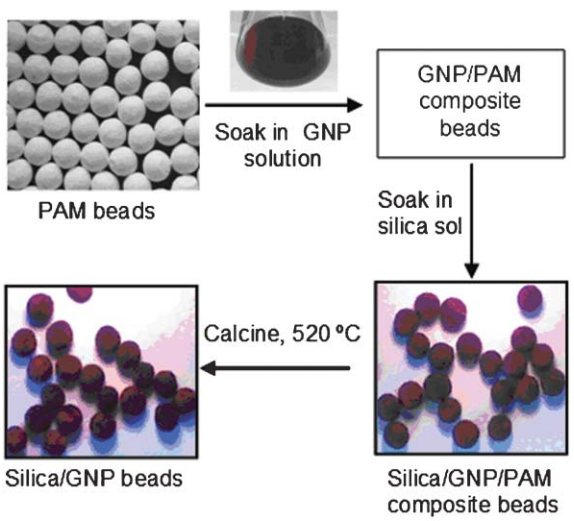

Fig. 1 Scheme for the preparation of hierarchically-porous GNP–silica composite beads (average bead diameter = 2.0 mm).

[a]*Donnan and Robert Robinson Laboratories, Department of Chemistry, University of Liverpool, Crown Street, Liverpool, UK L69 3BX. E-mail: zhanghf@liv.ac.uk*
[b]*National Institute for Biotechnology & Genetic Engineering (NIBGE), PO Box 577, Jhang Road, Faisalabad, Pakistan*

† Electronic supplementary information (ESI) available: Synthesis of the materials, characterization details, SEM images, and BET data. See DOI: 10.1039/b604392e

room temperature for 12 h, the composite beads were placed in an oven at 60 °C and 120 °C each for 24 h to allow the completion of the silica sol–gel process. The mass of the silica–GNP–PAM composites was 110% higher than the mass of the PAM beads. No change in the colour of the beads was observed, suggesting that the sol–gel process did not cause the GNPs to aggregate.[15] The silica–GNP–PAM composite beads were then calcined at 520 °C in air for 4 h to remove the organic PAM phase.[16,17] The inorganic beads obtained at the end of the calcination were also red in colour (Fig. 1), again suggesting that the GNPs were not aggregated despite the prolonged heat treatment.

Scanning electron microscope (SEM) imaging showed that the highly-interconnected emulsion-templated macropore structure of the original PAM beads was retained in the silica–GNP–PAM composites (images not shown). Some shrinkage was observed after calcination for the red GNP–silica beads (a reduction of approximately 35% in the original diameter, 1.5 mm), which is in accordance with our previous observation for pure silica beads.[17] Fig. 2a shows the porous structure of a cross-sectioned GNP–silica bead after calcination. The macropores are distributed across the whole bead and the interconnected emulsion-templated pore structure is retained (see inset). Imaging at higher magnification showed multiple bright dots distributed uniformly throughout the silica matrix (Fig. 2b). At a still higher magnification (Fig. 2c), one can see clearly the discrete GNPs distributed throughout the mesopores of the silica structure. The average diameter of the gold nanoparticles as measured by SEM was around 15 nm, which is consistent with the diameter of the original GNPs used for this experiment as determined by TEM. We estimated the loading of gold nanoparticles in these GNP–silica composite beads to be around 15 wt% based on gravimetric measurement. This is a relatively high metal loading, especially when one considers that there is no evidence of gold particle aggregation or sintering in the SEM images (Fig. 2c). In principle, the loading of gold nanoparticles in the porous silica could be increased to about 50 wt% as we have shown that the loading of GNPs on PAM beads can be increased further.[14] It may, however, become more difficult to prevent gold particle aggregation at higher metal loading.

The apparent Brunauer–Emmett–Teller (BET) surface area for the original PAM beads was found to be low (15 $m^2\ g^{-1}$). By contrast, the N_2 adsorption curve for the calcined silica–GNP composites (see Supporting Information, Fig. S1†) rises abruptly at low relative pressure (P/P_0) and the isotherm can be classed as Type I—that is, the material exhibits significant microporosity.[18] The apparent BET surface area for the silica–GNP material was determined to be 383 $m^2\ g^{-1}$, of which the micropore surface area constituted 297 $m^2\ g^{-1}$. By comparison, silica beads generated without the inclusion of GNPs by a similar (though not identical) procedure showed a somewhat lower surface area of 260 $m^2\ g^{-1}$ and a micropore surface area of 144 $m^2\ g^{-1}$.[17] The vast majority of the meso/micropores for these GNP–silica beads are less than 10 nm in diameter, as characterized by N_2 sorption analysis and calculated from the N_2 adsorption data using the Barrett, Joyner and Halenda (BJH) method.[19] A large proportion of these pores are less than 4 nm in diameter (Fig. S2†). The cumulative pore volume of N_2 adsorption (*i.e.* excluding the emulsion templated macropores) was found to be 0.16 $cm^3\ g^{-1}$ for the pure silica beads while the pore volume for the GNP–silica beads was found to be just 0.022 $cm^3\ g^{-1}$. It is possible that the GNPs occupy or obstruct a significant proportion of the mesopore/micropore volume while still contributing to the overall surface area for the composite material.

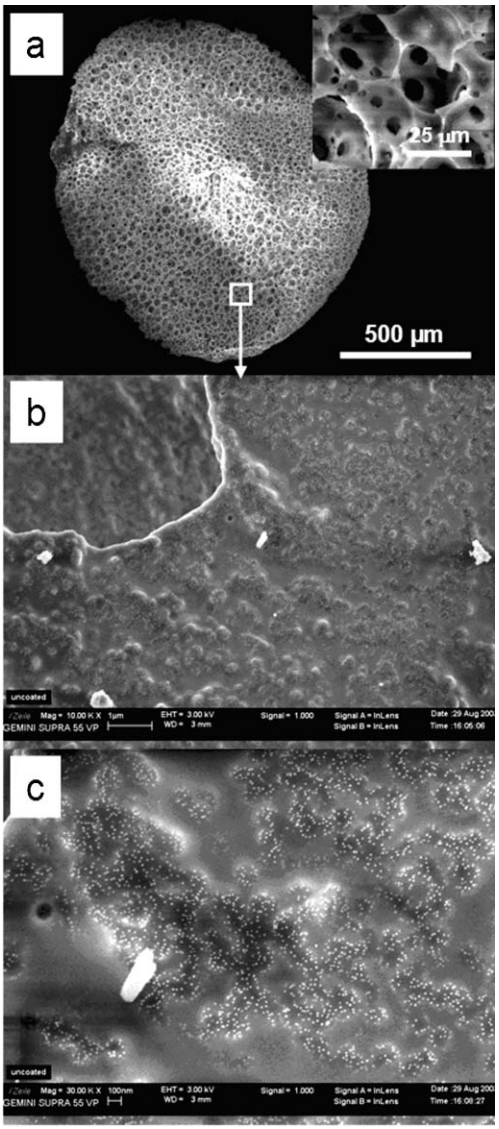

Fig. 2 SEM images of a GNP–silica bead. (a) The porous structure of the cross-sectioned surface and the highly interconnected emulsion-templated pores (inset). (b) Multiple bright spots observed on the silica matrix. (c) The discrete gold nanoparticles dispersed in the silica.

This method for the preparation of porous GNP–silica nanocomposites has readily been extended to the preparation of other porous GNP–metal oxide materials. For example, GNP–alumina composite beads were prepared by an analogous procedure. The main difference in this preparation was that the wet GNP–PAM beads were washed using isopropanol and allowed to dry in air after the GNPs had been adsorbed. These GNP–PAM beads were then soaked in aluminium tri-*sec*-butoxide—acetone solution overnight at room temperature. The GNP–alumina beads were also uniformly red, which again indicates the presence of discrete gold nanoparticles in the composite. Fig. 3a shows an SEM image of the porous structure of a cross-sectioned GNP–alumina bead. At higher magnification,

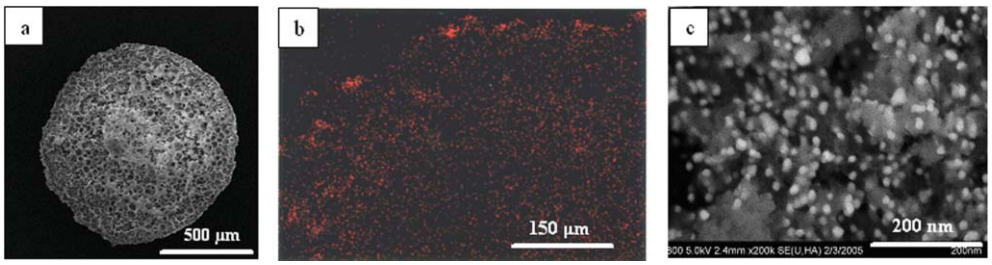

Fig. 3 (a) SEM image of a single cross-sectioned alumina–GNP composite bead; (b) EDX map of about a quarter of the bead shown in (a); (c) SEM image shows the presence of gold nanoparticles.

it was observed that the emulsion-templated macropores were well interconnected (Fig. S3†). To confirm that the gold was uniformly distributed in the alumina matrix, an EDX (Energy Dispersive X-ray microanalysis) analysis was carried out on one quarter of the bead shown in Fig. 3a. The presence of the element gold is mapped in red in Fig. 3b. One can see that the gold is quite uniformly distributed across the analyzed area. An aluminium map (Fig. S4†) shows the uniform aluminium distribution and the macropore structure. It is not possible to distinguish individual gold nanoparticles from the map shown in Fig. 3b since this analysis was carried out at a low magnification. However, a SEM image at a high magnification shows clearly the presence of discrete gold nanoparticles (Fig. 3c). The spherical shape of the nanoparticles can be observed in this image (diameter of particles = 15 nm) and it is clear that the GNPs tend to be partially embedded in the alumina matrix. This morphology suggests that the gold nanoparticles may be at least partly accessible to other molecules. The site-isolated nanomorphology also explains the lack of particle aggregation observed during sintering since, just as in the silica case described above, it is unlikely that these partially imbedded GNPs could have sufficient mobility for aggregation to occur. This is in strong contrast to our previous observations with organic PAM templates where complete agglomeration occurs to generate macroporous bulk metallic gold.[14]

Other metal nanoparticles (*e.g.*, palladium, platinum and rhodium) might also be used for the preparation of hierarchically porous nanocomposites in a similar fashion. For example, we have shown that palladium nanoparticles stabilized by 4-dimethyamino pyridine (DMAP) could also be adsorbed into emulsion-templated macroporous PAM beads. A similar procedure was then followed to prepare an analogous palladium–silica nanocomposite. In this case, the calcining process was carried out in a nitrogen atmosphere instead of in air. A detailed investigation is in progress to test the site isolation of the palladium particles and to investigate the use of these materials as catalysts for chemical reactions (*e.g.* Suzuki or Heck coupling reactions).

In conclusion, we describe here a versatile new route to prepare hierarchically porous composites containing site-isolated metal nanoparticles. These materials contain emulsion-templated macropores which could enhance mass transport, especially for large biomacromolecules or in viscous reaction systems. The macropore "highways" are interconnected with micro/mesopores to allow easy access to the active sites. Importantly, these materials can be produced with a high loading of site-isolated metal nanoparticles (15 wt%). We believe that the organic stabilizers at the surface of nanoparticles can be removed during the calcination process to result in the immobilization of naked metal nanoparticles in the porous inorganic oxide matrix which may be catalytically active for various chemical reactions. Composites of this type are currently being investigated in a range of catalytic applications, and we believe that this strategy may be particularly valuable for generating multifunctional supports for cascade reaction processes.

This work was supported by EPSRC (EP/C511794/1). HZ is a RCUK Academic Fellow. AIC is a Royal Society University Research Fellow. IH thanks NIBGE and the Ministry of Science & Technology, the Government of Pakistan for funding.

Notes and references

1 S. Behrens and G. Spittel, *Dalton Trans.*, 2005, 868.
2 S. Yoda, A. Hasegawa, H. Suda, Y. Uchimaru, K. Haraya, T. Tsuji and K. Otake, *Chem. Mater.*, 2004, **16**, 2363.
3 A. K. Sinha, S. Seelan, S. Tsubota and M. Haruta, *Angew. Chem., Int. Ed.*, 2004, **43**, 1546.
4 M. Brust, M. Walker, D. Bethell, D. J. Schiffrin and R. Whyman, *J. Chem. Soc., Chem. Commun.*, 1994, 801.
5 I. Hussain, M. Brust, A. J. Papworth and A. I. Cooper, *Langmuir*, 2003, **19**, 4831.
6 B. Rodriguez-Gonzalez, V. Salgueirino-Maceira, F. Garcia-Santamaria and L. M. Liz-Marzan, *Nano Lett.*, 2002, **5**, 471.
7 T. F. Baumann and J. H. Satcher, Jr., *Chem. Mater.*, 2003, **15**, 3745.
8 Y. Jiang and Q. Gao, *J. Am. Chem. Soc.*, 2006, **128**, 716.
9 (*a*) A. Imhof and D. J. Pine, *Nature*, 1997, **389**, 948; (*b*) H. Zhang and A. I. Cooper, *Soft Matter*, 2005, **1**, 107; (*c*) N. R. Cameron, *Polymer*, 2005, **46**, 1439.
10 H. Zhang and A. I. Cooper, *Chem. Mater.*, 2002, **14**, 4017.
11 A. K. Sinha, S. Seelan, S. Tsubota and M. Haruta, *Top. Catal.*, 2004, **29**, 95.
12 M. D. Hughes, Y. Xu, P. Jenkins, P. McMorn, P. Landon, D. I. Enache, A. F. Carley, G. A. Attard, G. J. Hutchings, F. King, E. H. Stitt, P. Johnston, K. Griffin and C. J. Kiely, *Nature*, 2005, **437**, 1132.
13 Z. Y. Yuang and B. L. Su, *J. Mater. Chem.*, 2006, **16**, 663.
14 (*a*) H. Zhang, I. Hussain, M. Brust and A. I. Cooper, *Adv. Mater.*, 2004, **16**, 27; (*b*) H. Zhang and A. I. Cooper, *J. Mater. Chem.*, 2005, **15**, 2157.
15 R. Elghanian, J. J. Storhoff, R. C. Mucic, R. L. Letsinger and C. A. Mirkin, *Science*, 1997, **277**, 1078.
16 H. Zhang, G. C. Hardy, M. J. Rosseinsky and A. I. Cooper, *Adv. Mater.*, 2003, **15**, 78.
17 H. Zhang, G. C. Hardy, Y. Khimyak, M. J. Rosseinsky and A. I. Cooper, *Chem. Mater.*, 2004, **16**, 4245.
18 K. S. W. Sing, D. H. Everett, R. A. W. Haul, L. Moscou, R. A. Pierotti, J. Rouquerol and T. Siemieniewska, *Pure Appl. Chem.*, 1985, **57**, 603.
19 It should be noted that the BJH method is based on macroscopic thermodynamic models, and BJH-derived pore sizes, though often quoted in the literature, should be regarded as "apparent" rather than definitive. The use of this methodology as an approximation can be defended since a number of studies show that pore sizes calculated using the BJH method tend to fall in the right range, see: M. Thommes, R. Kohn and M. Froba, *J. Phys. Chem. B*, 2000, **104**, 7932 and references therein. The BJH method is also used here in order to make a direct comparsion with our previous studies[17].